Available online at www.sciencedirect.com

SciVerse ScienceDirect

Ceramics International 38 (2012) 6889–6893

CERAMICS INTERNATIONAL

www.elsevier.com/locate/ceramint

Short communication

Macroporous sol–gel bioglasses scaffold with high compressive strength, porosity and specific surface area

Na Li[a,*], Ruoding Wang[b]

[a]Center for Clean Energy Engineering, University of Connecticut, 44 Weaver Road, Unit 5233, Storrs, CT 06269, USA
[b]Shanghai Institute of Ceramics, Chinese Academy of Sciences, 1295 Dingxi Road, Shanghai 200050, China

Received 29 July 2011; received in revised form 12 April 2012; accepted 23 April 2012
Available online 9 May 2012

Abstract

Bioactive glasses are known to have the ability to regenerate bone, but their use has been restricted mainly to powder, granules, or small monoliths. In this work, a series of macroporous bioglasses were produced by adding dried steamed bread particles into the sol as pore former. The porosity and macroporous diameter can be controlled by altering the particle size and volume of pore former. The macroporous structure can provide the potential room for tissue ingrowth. Simultaneously the samples exhibit mesoporous texture and high specific surface which can enhance bioactivity and release of ionic products. The most important is that these samples show satisfactory mechanical strength. These materials can fulfill the demands of scaffolds for bone tissue engineering and have great potential in applications to repair and reconstruct damaged tissue.

Keywords: A. Sol–gel processes; B. Porosity; C. Strength; D. Glass

1. Introduction

The macroporous sol–gel bioglasses with pore size over 100 μm should be the ideal scaffold for bone tissue engineering applications. Since sol–gel biogasses have excellent bioactivity, which can form chemically strong bond with bone; they can supply good interface for cell, should be beneficial to cell proliferation and differentiation; most importantly they can cause the rapid expression of genes and the production of growth factors [1]. The macroporous structure (greater than 100 μm) can ensure tissue ingrowth and nutrient delivery to the center of the regenerated tissue [2], the inherent mesoporous structure (2–50 nm) of the sol–gel materials can promote cell adhesion, adsorption of biological metabolites, bioactivity and degradability at controlled rates to match that of tissue repair [3–6]. An ideal scaffold should combine the beneficial properties of bioactive glasses with a hierarchical structure consisting of an interconnected network with macropores and mesopores simultaneously.

However, it is difficult to produce highly porous sol–gel glasses with pore diameter above 100 μm because the great shrinkage of gel during drying procedure often results in severe cracks. Most of the technologies can only produce the pores under 10 μm [7–9]. Recently a few attempts have been made to produce macroporous bioglasses for scaffolds. These attempts include foaming method that use $Ca(HCO_3)_2$ [10] to create bubbles or surfactants to produce sol foams [4]; pore former method that use PVA [11], PEG [12] to leave pores in the sintering process; and solid freeform fabrication techniques [13,14]. All these researches did not mention much about mechanical strength. However, certain mechanical strength is essential to scaffold materials, it should provide the needed early strength to the implant while tissue regeneration was occurring [15,16].

In this paper, macroporous sol–gel bioglasses were produced using steamed bread particles as pore formers under high humidity drying condition. The samples showed high mechanical strength. The nitrogen adsorption and desorption analysis revealed the materials had typical mesoporous characterization and high specific surface

*Corresponding author. Tel.: +1 860 486 9068; fax: +1 860 486 4745.
E-mail addresses: nali@engr.uconn.edu, bluegrape2008@gmail.com (N. Li).

0272-8842/$36.00
http://dx.doi.org/10.1016/j.ceramint.2012.04.061

area, SEM observation and mercury intrusion test showed that the materials had controllable macroporous structure.

2. Experiment

The chosen composition was bioactive glass 58S (SiO_2 58 wt%, CaO 33 wt%, and P_2O_5 9 wt%) [17]. The procedures were similar to those used by Zhong et al. [18]. Briefly, the 58S sol was prepared by mixing distilled water, HNO_3 (2 M), tetraethoxysilane, triethylphosphate; and calcium nitrate tetra-hydrate in order. The sols were aged in a drying oven at 60 °C to reach the high enough viscosity. Then the prepared pore formers were added into them with strong stirring for mixing uniformly. After aging at 60 °C for one day, the gels were moved into drying vessels. The drying method is followed according to [19]. They were dried in an environment containing 50: 50% mixtures of water/ethanol; the temperature was raised to 120 °C slowly and kept for 48 h. Finally the dried gels were sintered to 700 °C over 2 days.

The steamed bread was dried, ground and sieved before experiment and two size ranges (S=150–200 μm and M=200–315 μm) were selected for pore former. Two particle/sol ratios (weight of pore formers/volume of sol=0.8 g/20 mL and 1.1 g/20 mL) were used for each particle size. As-produced samples were labeled as M–X–Y, where M represent the pore former, X and Y represent pore former size and weight respectively. And the 58S sol–gel bioglasses without any pore formers were produced to be control samples BG00.

Pellets were characterized by using scanning electron microscopy (SEM), N_2 absorption isotherm, Mercury Intrusion porosimetry analyses and mechanical test. The microstructure was observed by an electron probe X-ray microanalyser (EPMA-8705QH_2, Shimadzu, Japan), on samples sputter coated with Au. Specific surface area and mesopore size distribution was calculated from the N_2 absorption isotherm by using the BET method in a Micromeritics Tristar 3000. Macropore size distribution and porosity was determined in a Micromeritics Poresizer 9320. Large and total pore results were measured from pressure 0 to 25 psi (the macro results) and 0–30000 psi (the total results) respectively. Apparent porosity was determined using the Archimedes' principle. The linear shrinkage was calculated based on the diameter of the sample at different stages such as before drying, after drying, and after sintering. The compressive strength measurement was conducted with a mechanical tester at 0.5 mm/min crosshead speed (INSTRON 8501) according to the JIS R1601 standard. Five samples of each kind were tested and the standard deviation was calculated.

3. Results and discussion

Flawless macroporous sol–gel bioglasses can be produced with different pore sizes and porosities. A wide range of shapes and sizes was attained with different molds, with no evidence of heterogeneities or phase separation, demonstrating the techniques' reliability.

Table 1 compares the shrinkage of the different kinds of samples during the heat treatment process. The pore formers in the gel prevent the shrinkage of whole gels to a certain extent. The BG00 sample has the maximum shrinkage 52%, and the macroporous samples have the average shrinkage only about 44%. Additionally, there is a relation between the shrinkage and the pore former/sol ratio, but there is no obvious relation between the shrinkage and the size of the pore formers. The bigger is the pore former/sol ratio, the smaller is the shrinkage. The samples having the same pore former/sol ratio have almost the same amount of linear shrinkage.

N_2 adsorption–desorption isotherms and the pore size distribution of the samples are shown in Fig. 1. The BET data for BG00 and macroporous materials are presented in Table 2. The macroporous samples exhibited a mesoporous network (average diameter of 3.3–3.9 nm) with a high specific surface area of 342–421 $m^2\,g^{-1}$. The isotherms were ascribed to type IV, according to the BDDT classification originally proposed by Brunaer and coworkers, which are characteristic of mesoporous (2–50 nm pore diameter) materials. The isotherms exhibit type H_2 hysteresis loops in the mesoporous range, which are characteristic of the so-called ink bottle pores that have pore cavities larger in diameter than the openings (throats) leading into them [17]. There is not much difference of the hysteresis loops character between BG00 and macroporous samples, and all the samples showed the mesopore diameter range below 6 nm, the average pore diameter is similar, so the pore formers almost remain the mesoporous structure of 58S sol–gel glasses. While compared to BG00 samples, the specific surface area (S_p) and the pore volume (V_p) of macroporous samples increased obviously, S_p and V_p

Table 1
Process parameter of the macroporous specimens prepared in this work, data of sample linear shrinkage and macroporous structure measured by mercury intrusion porosimetry.

Designation	Pore former particles size (μm)	Particle/sol ratio ($g\,ml^{-1}$)	Average pore diameter (μm)	Total pore volume ($cm^3\,g^{-1}$)	Linear shrinkage (%)
M-S-0.8	150–200	0.040	16.6	0.22	44.7
M-S-1.1	150–200	0.055	13.0	0.37	42.5
M-M-0.8	200–315	0.040	20.8	0.19	45.2
M-M-1.1	200–315	0.055	14.7	0.25	42.6

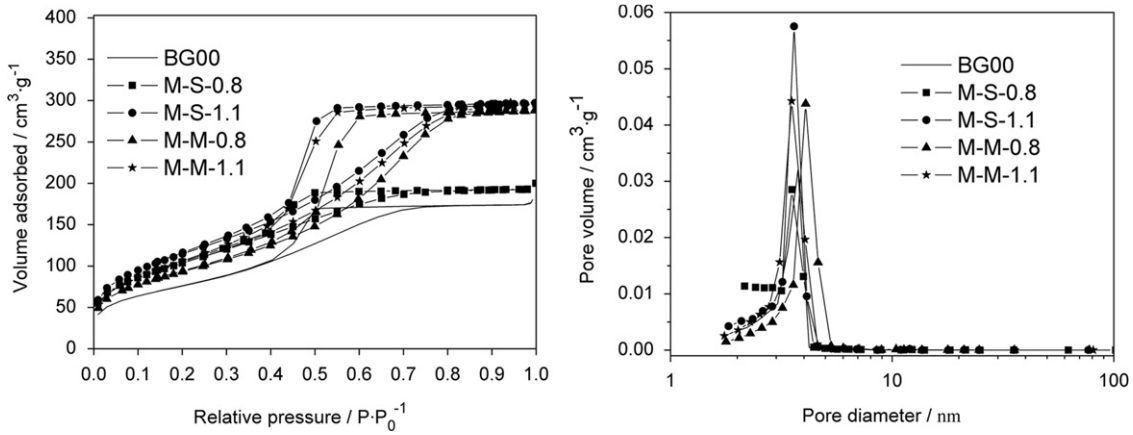

Fig. 1. Nitrogen adsoption–desorption isotherms and the corresponding pore-size distribution.

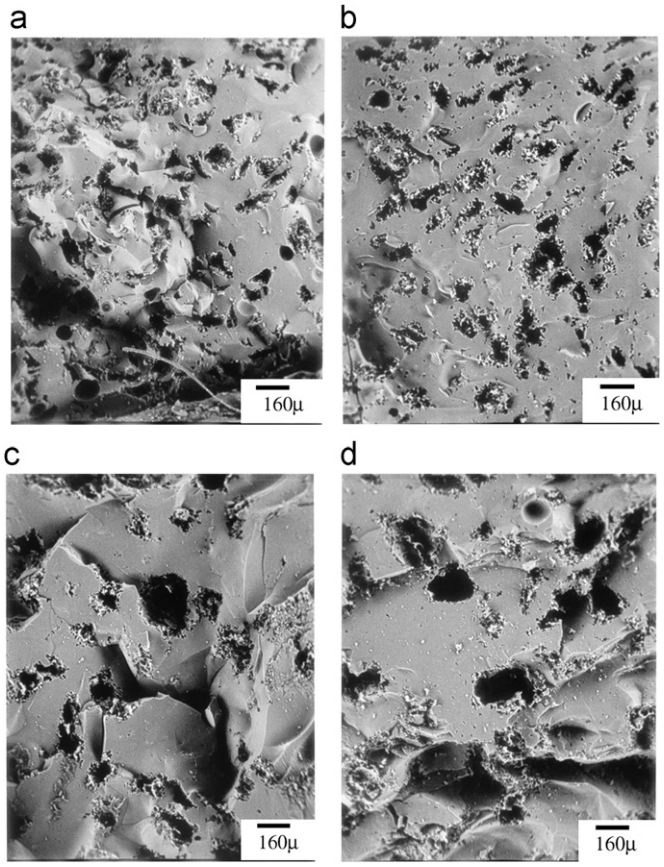

Fig. 2. The microstructure of macroporous samples observed by SEM. (a) M-S-0.8, (b) M-S-1.1, (c)M-M-0.8 and (d) M-M-1.1.

increased with the pore former volume while there is no remarkable relation to the pore former size.

Fig. 2 shows the SEM microstructure of the cross-section of macroporous bioglasses. Most of the pores are larger than 50 μm and they are irregular circular open pores. The distribution of the pores is homogeneous. We can see the influence of particle size of the pore former on the pore size distribution clearly. The larger particle size resulted in larger pores. And, the larger bread volume resulted in greater pore volume. There are some smaller pores on the sample cross section beside big pores. The diameters of these smaller pores vary from 1 to 10 μm. They may come from the bread dissolved into sol during the mixing procedure. A part of bread precipitated from sol during the drying process and left the smaller pores in the specimens after burning out.

The SEM micrographs provided qualitative information on the material structure, while mercury porosimetry allowed a quantitative investigation of the porosity [20]. Fig. 3 compared the pore volumes and pore size distribution of the specimens measured by mercury intrusion porosimetry. Mercury intrusion porosimetry is usually used to measure the smaller pores, corresponding to the connecting areas or necks between much larger pores created by bread particles [20]. So the true porosity and pore diameter values should be higher. The calculated macropore diameter and total pore volume of various samples are given in Table 1. The results are in accord with the trend of macropore structure observed by SEM. The larger is the bread particle, the bigger is the pore size. And, the larger is the bread volume, the greater is the pore volume. But for the samples added with same bread volume, the larger bread size resulted in the smaller pore volume. This pore volume result agrees with the apparent porosity measured using Archimede's principle (Fig. 4). Namely, the porosity of M-M-0.8 is smaller than that of M-S-0.8, and the porosity of M-M-1.1 is smaller than that of M-S-1.1. The porosity of the samples with same pore former volume should be same theoretically; however there is a decrease when the pore former particle size increased, it may be due to the high solubility of the large bread particles in the sols.

Fig. 4 shows compressive strength and the apparent porosity of the obtained samples. All the macroporous samples show large porosity (54–65%) and high strength simultaneously, and the strength are higher than that of human cancellous bone (2–10 MPa). The high strength of these materials is beneficial to withstand physiological stresses and minimize stress shielding in the surrounding host bone [16]. The strength decreased with the increase of

Table 2
Data of mesoporous structure measured by nitrogen sorption analysis.

Designation	Specific surface area ($m^2\ g^{-1}$)	Specific pore volume ($cm^3\ g^{-1}$)	Average pore diameter (nm)
BG00	276	0.29	3.4
M-S-0.8	380	0.35	3.3
M-S-1.1	421	0.48	3.4
M-M-0.8	342	0.46	3.9
M-M-1.1	381	0.48	3.4

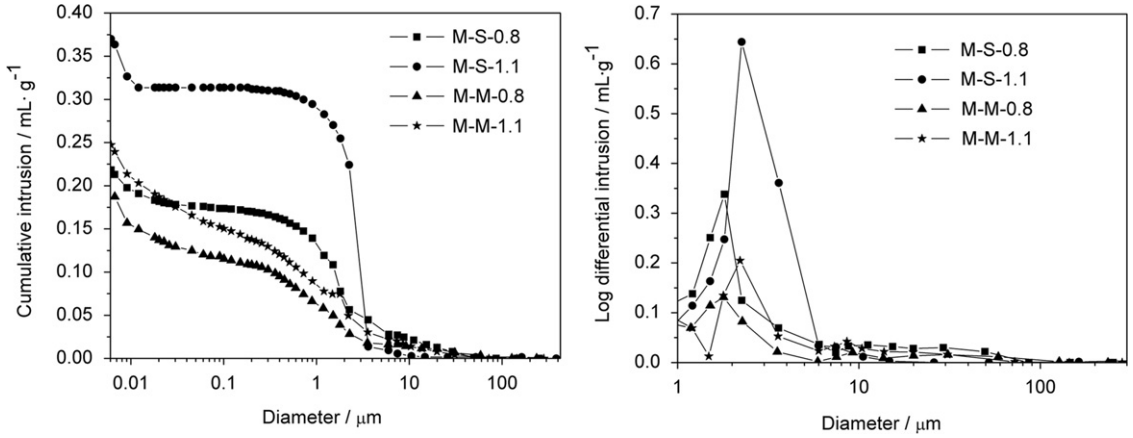

Fig. 3. Mercury porosimetry curves for macroporous bioglass.

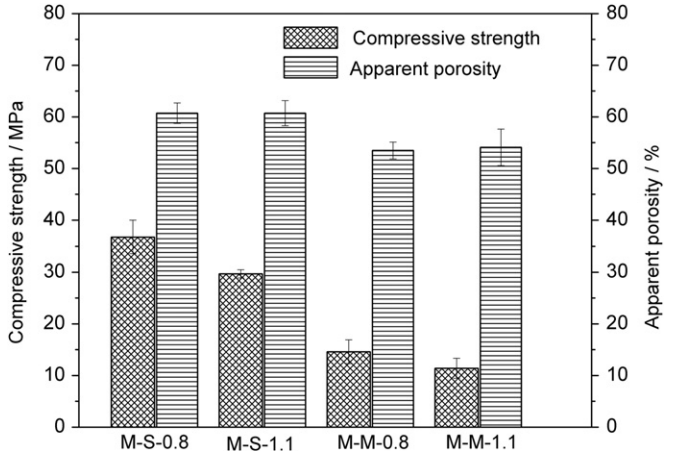

Fig. 4. Compressive strength and apparent porosity of the macroporous samples.

the pore former size and volume, especially the pore former size. The results verified the microstructure, porosity and pore size distribution are in direct relationship with the strength.

Due to the intense evaporation of water and ethanol with the shrinkage of the volume, the severe crack often occurred in sol–gel process. A solid pore former added into gel will prevent the shrinkage of gel. So BG00 sample has the maximal shrinkage and probability to crack. Using the improper pore former, the gel structure was loosened even if the severe crack did not occur. The steamed bread particle is an appropriate pore former according to the fact that the samples are in good condition and showed very high compressive strength. The steamed bread has several characters as an appropriate pore former. First, it has similar density to the sols and can be dispersed into the sols homogeneously without sedimentation. Second, it has good swelling property and good affinity for gel particles, which keep the compact gel structure and a high mechanical strength. Third, the macropore size and porosity can be controlled by the different particle size and volume of the steamed bread.

4. Conclusions

In this work, sol–gel and pore former technologies were combined to create a hierarchical structural bioglasses composed of macropores (above 50 μm) and mesopores (2–6 nm). Using this method, it is easy to control pore diameter and volume by using bread particles with different size range and volume. Moreover, the samples showed high strength (11.4–36.8 MPa) and specific surface area (342–421 $m^2\ g^{-1}$). These macroporous materials potentially can support organization of cells, and resorb by

controlled rates, is promising to serve as 3D cell scaffold for bone tissue engineering.

References

[1] I.D. Xynos, A.J. Edgar, L.D.K. Buttery, L.L. Hench, J.M. Polak, Ionic dissolution products of bioactive glass increase proliferation of human osteoblasts and induce insulin-like growth factor II mRNA expression and protein synthesis, Biochemical and Biophysical Research Communications 276 (2000) 461–465.

[2] T.M. Freyman, I.V. Yannas, L.J. Gibson, Cellular materials as porous scaffolds for tissue engineering, Progress in Materials Science 46 (2001) 273–282.

[3] J.R. Jones, L.L. Hench, Factors affecting the structure and properties of bioactive foam scaffolds for tissue engineering, Journal of Biomedical Materials Research Part B: Applied Biomaterials 68B (2004) 36–44.

[4] P. Sepulveda, J.R. Jones, L.L. Hench, Bioactive sol–gel foams for tissue repair, Journal of Biomedical Materials Research 59 (2002) 340–348.

[5] E. Charrière, J. Lemaitre, Ph. Zysset, Hydroxyapatite cement scaffolds with controlled macroporosity: fabrication protocol and mechanical properties, Biomaterials 24 (2003) 809–817.

[6] H. Yoshimoto, Y.M. Shin, H. Terai, J.P. Vacanti, A biodegradable nanofiber scaffold by electrospinning and its potential for bone tissue engineering, Biomaterials 24 (2003) 2077–2082.

[7] K. Nakanishi, Porous gels made by phase separation: recent progress and future directions, Journal of Sol–Gel Science and Technology 19 (2000) 65–70.

[8] H. Shikata, K. Nakanishi, K. Hirao, Preparation of silicalite-1 within macroporous silica glass, Journal of Sol–Gel Science and Technology 19 (2000) 769–773.

[9] H. Yan, K. Zhang, C.F. Blanford, L.F. Francis, A. Stein, In vitro hydroxycarbonate apatite mineralization of $CaO–SiO_2$ sol–gel glasses with a three-dimensionally ordered macroporous structure, Chemistry of Materials 13 (2001) 1374–1382.

[10] S.R. Hall, D. Walsh, D. Green, R. Oreffo, S. Mann, A novel route to highly porous bioactive silica gels, Journal of Materials Chemistry 13 (2003) 186–190.

[11] Q. Jie, K.L. Lin, J.P. Zhong, Y. Shi, Q. Li, J. Chang, R. Wang, Preparation of macroporous sol–gel bioglass using PVA particles as pore former, Journal of Sol–Gel Science and Technology 30 (2004) 49–61.

[12] N. Li, Q. Jie, S. Zhu, R. Wang, Preparation and characterization of macroporous sol–gel bioglass, Ceramics International 31 (2005) 641–646.

[13] S. Padilla, S. Sánchez-Salcedo, M. Vallet-Regí, Bioactive glass as precursor of designed-architecture scaffolds for tissue engineering, Journal of Biomedical Materials Research 81A (2007) 224–232.

[14] H. Yun, S. Kim, Y. Hyeon, Design and preparation of bioactive glasses with hierarchical pore networks, Chemical Communications 21 (2007) 2139–2141.

[15] H.H.K. Xu, J.B. Quinn, S. Takagi, L.C. Chow, Synergistic reinforcement of in situ hardening calcium phosphate composite scaffold for bone tissue engineering, Biomaterials 25 (2004) 1029–1037.

[16] J.M. Karp, P.D. Dalton, M.S. Shoichet, Scaffolds for tissue engineering, Materials Research Society Bulltein 28 (2003) 301–306.

[17] L.L. Hench, J.K. West, Biological applications of bioactive glasses, Life Chemistry Reports 13 (1996) 187–241.

[18] J.P. Zhong, D.C. Greenspan, Processing and properties of sol–gel bioactive glasses, Journal of Biomedical Materials Research 53 (2000) 694–701.

[19] J.P. Zhong, D.C. Greenspan, Porous sol–gel bioglass from near-equilibrium drying, in: Rey Sedel (Ed.), Bioceramics, 10, Elsevier Science, New York, 1997, pp. 265–268.

[20] R.F.S. Lenza, W.L. Vasconcelos, J.R. Jones, L.L. Hench, Surface-modified 3D scaffolds for tissue engineering, Journal of Materials Science: Materials in Medicine 13 (2002) 837–842.